ELSEVIER

International Journal of Thermal Sciences 41 (2002) 927–935

International Journal of Thermal Sciences

www.elsevier.com/locate/ijts

Simultaneous heat and mass transfer of a packed distillation column for ammonia–water absorption refrigeration systems

José Fernández-Seara *, Jaime Sieres, Manuel Vázquez

Área de Máquinas y Motores Térmicos, Escuela Técnica Superior de Ingenieros Industriales de Vigo,
Universidad de Vigo, Campus Lagoas-Marcosende, N° 9, 36200 Vigo, Spain

Received 21 July 2001; accepted 1 November 2001

Abstract

This paper presents a study on the NH_3–H_2O distillation process using a packed column with liquid reflux from the condenser in an absorption refrigeration system. A differential mathematical model has been developed on the basis of mass and energy balances and the heat and mass transfer equations. A net molar flux between the liquid and vapour phases has been considered in the mass transfer equation, which obviates the need to assume equimolar counter-diffusion. The model equations have been solved using the finite-difference method. Results obtained for a specific application are shown, including parameter distributions along the column length. The influence of rectifying and stripping lengths, mass and heat transfer coefficients and volumetric heat rejection from the column, on the distillate ammonia concentration has been analysed.

Keywords: Packed distillation column; Ammonia–water; Absorption refrigeration; Heat transfer; Mass transfer

---

1. Introduction

Sorption systems have been the object of an increasing interest in recent years. This is contributing to a renewal of their technology, a consolidation of their classic applications and an expansion of their use into new fields. However, with regard to working pairs, and despite of the new mixtures under investigation, only the two classical pairs H_2O–BrLi and NH_3–H_2O prevail with a clear future [1].

In the field of refrigeration, ammonia–water has been the most widely used mixture from its beginning. Nevertheless, in spite of its widespread use and its many advantages, this pair exhibits some disadvantages. The main drawback is due to the fact that the vapour pressure of the sorbent (water) is not negligible as compared with the vapour pressure of the refrigerant (ammonia). Therefore, the vapour leaving the generator always contains a small fraction of water. The vapour water content must be reduced to a minimum, otherwise it tends to accumulate in the evaporator. The presence of water in the evaporator raises the evaporation temperature and strongly deteriorates the efficiency of the system. These effects are increased as the evaporation temperature decreases. Ignoring the water content of the regenerated vapour constitutes one of the major pitfalls in designing an ammonia–water refrigeration system, as pointed out by Bogart [2].

One way to diminish the water content of the vapour is reducing the carry over of water from the generator. This can be attained by adding a salt to the ammonia–water mixture. This procedure was first proposed by Altenkirch, as reported by Stephan, 1983 [3]. Nowadays, the seek for ingredients to be added into the solution in order to reduce the vapour pressure of water and thereby the need for vapour purification is an active research area [4–6]. However, up to now no commercial products have been made available. Therefore, in ammonia–water refrigeration systems a purification process to reduce the water content of the vapour leaving the generator is required. This can be achieved by using a rectifier or a distillation column, as stated by Herold et al., 1996 [7]. The design of an efficient device to carry out this purification process has become a crucial issue in designing ammonia–water absorption refrigeration systems.

This paper deals with the analysis of the purification process executed by means of a distillation column with

---

[*] Correspondence and reprints.
E-mail addresses: jseara@uvigo.es (J. Fernández-Seara), jsieres@uvigo.es (J. Sieres), mvazquez@uvigo.es (M. Vázquez).

1290-0729/02/$ – see front matter © 2002 Éditions scientifiques et médicales Elsevier SAS. All rights reserved.
PII: S1290-0729(02)01385-6

Nomenclature

A	transfer area	m^2
a_{ef}	effective transfer area	$\mathrm{m}^2\cdot\mathrm{m}^{-3}$
Cp	specific heat	$\mathrm{J}\cdot\mathrm{kg}^{-1}\cdot\mathrm{K}^{-1}$
D_{t}	column diameter	m
h	specific enthalpy	$\mathrm{J}\cdot\mathrm{kg}^{-1}$
Le	Lewis number	
M	molecular weight	$\mathrm{kg}\cdot\mathrm{kmol}^{-1}$
$\dot{M}$	mass flux transferred	$\mathrm{kg}\cdot\mathrm{m}^{-2}\cdot\mathrm{s}^{-1}$
$\dot{m}$	mass flow	$\mathrm{kg}\cdot\mathrm{s}^{-1}$
$\dot{N}$	molar flux transferred	$\mathrm{kmol}\cdot\mathrm{m}^{-2}\cdot\mathrm{s}^{-1}$
Pr	Prandtl number	
$\dot{q}$	sensible heat	W
$\dot{q}_{\mathrm{r}}$	volumetric heat rejection	$\mathrm{W}\cdot\mathrm{m}^{-3}$
$\dot{Q}$	heat load	W
Sc	Schmidt number	
T	temperature	K
x	ammonia mass concentration	$\mathrm{kg}\cdot\mathrm{kg}^{-1}$
xm	ammonia molar concentration	$\mathrm{kmol}\cdot\mathrm{kmol}^{-1}$
y	coordinate along the column	m
z	ammonia to total molar flux transferred ratio	

Greek symbols

α	heat transfer coefficient	$\mathrm{W}\cdot\mathrm{m}^{-2}\cdot\mathrm{K}^{-1}$
α_{m}	corrected heat transfer coefficient	$\mathrm{W}\cdot\mathrm{m}^{-2}\cdot\mathrm{K}^{-1}$
β	mass transfer coefficient	$\mathrm{kmol}\cdot\mathrm{m}^{-2}\mathrm{s}^{-1}$
λ	molar latent heat of vaporization	$\mathrm{J}\cdot\mathrm{kmol}^{-1}$

Subscripts

B	bottoms
C	condenser
D	distillate
F	feed conditions
G	generator
i	interface
l	liquid
r	reflux
top	top column conditions
v	vapour

total condensation. The schematic structure of a distillation column of this type, including the generator is depicted in Fig. 1. Heat is applied in the generator to produce a vapour stream that enters at the bottom of the distillation column and rises in counter-flow to a liquid stream, so that heat and mass transfer processes between both phases are enabled. These processes are enhanced by using a suitable contacting such as a packing material (packing columns) or a set of plates (plate columns). The contact zone over the feed entry point is known as the rectifying section and the one below as the stripping section, as shown in Fig. 1.

In the rectifying section the downwards liquid stream is called reflux. The reflux must be injected at the top of the column. It can be produced either by partial condensation of the vapour at the column top in a rectifier, or by returning part of the condensed liquid from the condenser. The former is usually denominated partial condensation and the latter complete condensation. In the stripping section the liquid stream is a mixture of the liquid column feed and the solution from the rectifying section. Therefore, the rising vapour is in heat and mass exchange with the liquid throughout the column, which causes a small fraction of vapour with a relatively high water concentration to condense, realising heat of condensation. This simultaneously, induces the evaporation of a fraction of the liquid solution which is essentially pure ammonia. Consequently the concentration of the vapour stream gradually increases as it flows towards the column top, meanwhile the liquid concentration decreases from top to bottom.

There is an extensive literature concerning the modelling of packed distillation columns by means of equilibrium stage models and HETP (height equivalent to a theoretical plate) stage efficiency concepts [8,9] but not much work has been reported on continuous or differential bases. Moreover, for most applications of binary distillation columns, the molar heats of vaporization of the components involved are similar, so that equimolar counter diffusion can be considered. However, for the ammonia–water mixture the heats of vaporization are considerably different and usually a net flux is established between the liquid and vapour phases. Furthermore, due to the temperature difference between both phases, heat transfer occurs simultaneously with mass transfer.

This paper presents a differential model for a packed distillation column with total condensation for an ammonia–water refrigeration system. The model has been implemented in a computer program, which provides the flow, temperature and concentration distributions of the vapour and liquid phases throughout the length of the tower, and investigates the column performance at various design and operating conditions. Similar models to the one presented here have been used to design components in ammonia water absorption systems. This technique was originally employed by Colburn and Drew [10] for the condensation of a binary vapour with a miscible condensate. Iedema [11] developed a model to study heat and mass transfer in the vapour and liquid phases of an ammonia water regenerator. Kang and Christensen [12] extended the model of Colburn and Drew to the design of counter-current vertical fluted tube absorbers. Kang et al. [13] developed a generalised component design model by combined heat and mass transfer analysis for ammonia–water absorption systems, obtaining a desorbed/absorbed vapour composition (z) map for each component with the direction of mass transfer. The same authors applied their model to a condenser with a fluted tube [14]

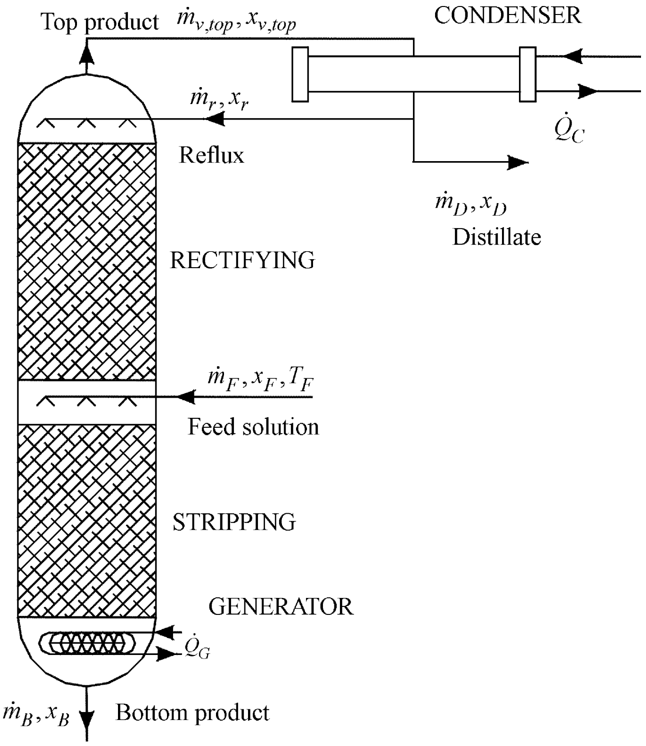

Fig. 1. Schematic diagram of the distillation column with total condensation.

and to a rectifier with different configurations [15]. Kang et al. [16] applied the model to a bubble absorber with a plate heat exchanger and Cao and Christensen [17] to a combined component absorber/desorber. Selim and Elsayed [18,19] recently presented a model for an ammonia–water packed absorber applying interfacial heat and mass transfer equations on the basis of packing mass transfer correlations.

2. Mathematical model

A model has been developed that takes into account combined heat and mass transfer processes in a packing distillation column. The mathematical model is based on the application of mass and energy balances and heat and mass transfer equations to a differential control volume, as shown in Fig. 2.

In formulating the model the following assumptions have been made:

(1) The processes are in steady state and the flow is one-dimensional.
(2) The pressure in the column is constant.
(3) Heat losses to the environment are neglected.
(4) The two-film and the Lewis and Whitman theory [20] of non-interfacial resistance are applied, i.e., equilibrium at the interface is considered.
(5) The heat and mass transfer areas are equal.
(6) The vapour stream and the liquid solution leaving the generator, located at the bottom of the column (Fig. 1), are in thermodynamic equilibrium.

2.1. Mass transfer equations

The mass transfer between the vapour and liquid phases results from the combined contribution of molecular diffusion and a bulk transport of material through the interface. A detailed discussion on the differential mass transfer equation and the boundary conditions used to determine the left and right terms of Eq. (1) are published in the literature [21–23]. The molar fluxes of ammonia transferred from the bulk vapour to the interface and from the interface to the bulk liquid are obtained as a function of the corresponding mass transfer coefficients (β), the molar bulk concentrations of ammonia and the ammonia molar concentrations at the interface. The molar flux is defined to be positive from the liquid to the vapour. The mass continuity requirement at the interface is established in Eq. (1), resulting in equal mass transport in the liquid and vapour phases.

$$\begin{aligned} \mathrm{d}\dot{N}_{\mathrm{NH_3}}|_{\mathrm{v}} &= \beta_{\mathrm{v}} \cdot z \cdot \ln\left(\frac{z - xm_{\mathrm{v}}}{z - xm_{\mathrm{vi}}}\right) \\ &= \beta_{\mathrm{l}} \cdot z \cdot \ln\left(\frac{z - xm_{\mathrm{li}}}{z - xm_{\mathrm{l}}}\right) = \mathrm{d}\dot{N}_{\mathrm{NH_3}}|_{\mathrm{l}} \end{aligned} \tag{1}$$

where, z is defined as the ratio of ammonia to the total molar flux, according to Eq. (2). The total molar flux, $\mathrm{d}\dot{N}$, is the sum of ammonia and water molar fluxes.

$$z = \frac{\mathrm{d}\dot{N}_{\mathrm{NH_3}}}{\mathrm{d}\dot{N}} \tag{2}$$

Colburn and Drew [10] defined the mass transfer coefficient (β) used in Eq. (1) for small mass transfer rates. However, the formulation of Eq. (1) is valid for any mass transfer rate. In this work, the mass transfer coefficients in the liquid and vapour phases have been obtained from the correlations reported by Onda et al. [24].

In mass transfer literature equimolar counter diffusion is usually considered in the distillation of binary mixtures [9, 22,25]. According to Trouton's rule, the molar enthalpy of vaporization is approximately constant for all components. Thus, if a fraction of the least volatile component of the vapour phase condenses then the same number of moles of the most volatile component will evaporate out of the liquid. However, the molar enthalpies of vaporization of ammonia and water are significantly different. Consequently, equimolar counter diffusion has not been considered in the formulation of the model and a bulk flow of material through the interface has been included in the mass transfer equation. Once the ammonia and the total molar fluxes are determined from Eqs. (1) and (2), then the corresponding mass fluxes can be obtained from Eqs. (3) and (4), where M is the component molecular weight.

$$\mathrm{d}\dot{M}_{\mathrm{NH_3}} = \mathrm{d}\dot{N}_{\mathrm{NH_3}} \cdot M_{\mathrm{NH_3}} \tag{3}$$

$$\mathrm{d}\dot{M} = \mathrm{d}\dot{N}_{\mathrm{NH_3}} \cdot M_{\mathrm{NH_3}} + \mathrm{d}\dot{N} \cdot (1 - z) \cdot M_{\mathrm{H_2O}} \tag{4}$$

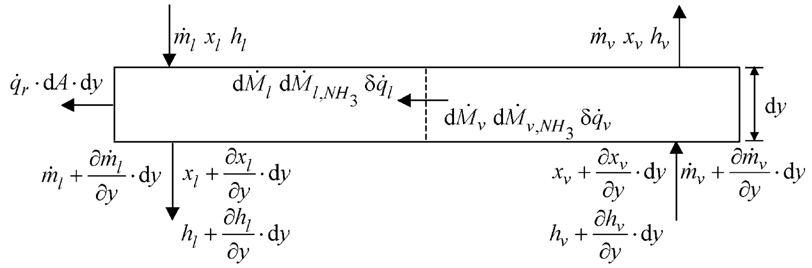

Fig. 2. Control volume for a differential packed section.

2.2. *Heat transfer equations*

Heat and mass transfer processes occur simultaneously in the liquid and vapour phases. Therefore, there is a sensible heat of the mass flux between the bulk and the interface conditions, which must be considered in the heat transfer equations. A detailed discussion of these equations can be found in the literature [21–23]. The sensible heats transferred from the bulk liquid to the interface and from the interface to the bulk vapour are given in Eqs. (5) and (6), respectively. As for the mass transfer equations, heat transfer is defined to be positive from the liquid to the vapour phase.

$$\delta\dot{q}_\mathrm{v} = \alpha_\mathrm{v} \cdot \frac{c_\mathrm{v}}{1 - e^{-c_\mathrm{v}}} \cdot (T_\mathrm{i} - T_\mathrm{v}) \cdot \mathrm{d}A \tag{5}$$

$$\delta\dot{q}_\mathrm{l} = \alpha_\mathrm{l} \cdot \frac{c_\mathrm{l}}{1 - e^{-c_\mathrm{l}}} \cdot (T_\mathrm{l} - T_\mathrm{i}) \cdot \mathrm{d}A \tag{6}$$

with c being

$$c = \frac{\mathrm{d}\dot{N}_{\mathrm{NH_3}} \cdot Cp_{\mathrm{NH_3}} + \mathrm{d}\dot{N}_{\mathrm{H_2O}} \cdot Cp_{\mathrm{H_2O}}}{\alpha} \tag{7}$$

The transfer area $\mathrm{d}A$ is given in Eq. (8), where a_ef is the effective transfer area obtained from Zarzycki and Chacuk [26], D_t is the column diameter and $\mathrm{d}y$ the length of the differential control volume.

$$\mathrm{d}A = a_\mathrm{ef} \cdot \frac{\pi \cdot D_\mathrm{t}^2}{4} \cdot \mathrm{d}y \tag{8}$$

The corrections applied in Eqs. (5) and (6) for the sensible heat change over the liquid and vapour films are equivalent to defining a modified heat transfer coefficient according to expression (9).

$$\alpha_\mathrm{m} = \alpha \cdot \frac{c}{1 - e^{-c}} \tag{9}$$

The value of α_m is greater than α if mass transfer is in the same direction as heat transfer. For a distillation column this is so if mass is transferred from the vapour to the liquid phase.

The coupled heat and mass transfer nature is also reflected in the energy balance (10) at the vapour–liquid interface, according to the control volume shown in Fig. 2. Eq. (10) states the energy continuity at the interface.

$$\begin{aligned}\alpha_\mathrm{lm} \cdot (T_\mathrm{l} - T_\mathrm{i}) &= \alpha_\mathrm{vm} \cdot (T_\mathrm{i} - T_\mathrm{v}) + \mathrm{d}\dot{N}_{\mathrm{NH_3}} \cdot \lambda_{\mathrm{NH_3}} \\ &\quad + \mathrm{d}\dot{N}_{\mathrm{H_2O}} \cdot \lambda_{\mathrm{H_2O}}\end{aligned} \tag{10}$$

where λ is the components molar latent heat of vaporization at the conditions of the interface.

Liquid and vapour heat transfer coefficients (α) are obtained using the Chilton and Colburn [27] analogy, which provides a relationship between heat and mass transfer coefficients, according to Eq. (11).

$$\alpha = Cp \cdot \beta \cdot \left(\frac{Sc}{Pr}\right)^{2/3} = Cp \cdot \beta \cdot Le^{2/3} \tag{11}$$

2.3. *Mass and energy balances*

Global mass, species and energy balances over the differential volume of packing with length $\mathrm{d}y$, as shown in Fig. 2, lead to Eqs. (12), (13) and (14).

$$\frac{\mathrm{d}\dot{m}_\mathrm{v}}{\mathrm{d}y} - \frac{\mathrm{d}\dot{m}_\mathrm{l}}{\mathrm{d}y} = 0 \tag{12}$$

$$\frac{\mathrm{d}(\dot{m}_\mathrm{v} \cdot x_\mathrm{v})}{\mathrm{d}y} - \frac{\mathrm{d}(\dot{m}_\mathrm{l} \cdot x_\mathrm{l})}{\mathrm{d}y} = 0 \tag{13}$$

$$\frac{\mathrm{d}(\dot{m}_\mathrm{v} \cdot h_\mathrm{v})}{\mathrm{d}y} - \frac{\mathrm{d}(\dot{m}_\mathrm{l} \cdot h_\mathrm{l})}{\mathrm{d}y} - \dot{q}_\mathrm{r} \cdot \mathrm{d}A = 0 \tag{14}$$

In Eq. (14) $\dot{q}_\mathrm{r}$ is the volumetric heat rejection from the packing of the column. A distillation column usually operates adiabatically, however the effect of a volumetric heat rejection has also been considered in order to evaluate its influence in the column performance.

An analysis of the bulk vapour phase yields Eqs. (15), (16) and (17). In Eq. (17) the vapour enthalpy of the mass transferred is the average value of the components vapour enthalpies at the interface temperature, as suggested by Webb [23], instead of the enthalpy of a vapour with z value of ammonia concentration. This formulation has been chosen taken into account that the mass transfer of ammonia and water in a distillation column usually occurs in opposite directions.

$$\mathrm{d}\dot{m}_\mathrm{v} = \mathrm{d}\dot{M} \cdot \mathrm{d}A \tag{15}$$

$$\mathrm{d}(\dot{m}_\mathrm{v} \cdot x_\mathrm{v}) = \mathrm{d}\dot{M}_{\mathrm{NH_3}} \cdot \mathrm{d}A \tag{16}$$

$$\begin{aligned}\mathrm{d}(\dot{m}_\mathrm{v} \cdot h_\mathrm{v}) &= \mathrm{d}\dot{M}_{\mathrm{H_2O}} \cdot h_{\mathrm{v,H_2O}} \cdot \mathrm{d}A \\ &\quad + \mathrm{d}\dot{M}_{\mathrm{NH_3}} \cdot h_{\mathrm{v,NH_3}} \cdot \mathrm{d}A + \delta\dot{q}_\mathrm{v}\end{aligned} \tag{17}$$

State equations used for the NH_3–H_2O equilibrium and thermodynamic properties are calculated from Ziegler and Trepp [28].

3. Solution method

The system of differential equations set previously has been solved using a finite difference numerical method. The column has been divided in a finite number of elements, n, with an incremental length, Δy. The iterative calculation was initiated at the top of the rectifying and stripping column sections.

3.1. Incremental element

If liquid and vapour conditions were known at the top section of any incremental element, then the conditions at the bottom section would be obtained. Calculation of the unknown conditions requires the determination of the mass and heat transferred between the liquid and vapour phases, which are obtained using Eqs. (1) to (11). As given by Eq. (1), mass transfer depends on the value of the ratio z and the interface molar concentrations xm_{li} and xm_{vi}, which are obtained from the interface temperature. On the other hand, the heat transfer given by Eqs. (5) and (6) depends on the interface temperature T_{i} and the ammonia and total mass transferred. For this reason, a trial and error procedure must be implemented to solve these equations.

The following algorithm uses two iterative loops to obtain the values of the interface temperature and the concentration ratio z. Once these parameters are calculated, the liquid and vapour conditions at the bottom section of any incremental element are computed. Thus, the input parameters for solving the next section are known. The mass and heat transfer coefficients and the transfer area are obtained from the input conditions and assumed constant throughout the incremental element. The calculation procedure in each element is summarised as follows:

(1) Guess the interface temperature.
(2) Calculate xm_{li} and xm_{vi} with the assumed temperature and column pressure.
(3) Guess z.
(4) Calculate $\Delta\dot{N}_{\mathrm{NH_3}}|_{\mathrm{v}}$ and $\Delta\dot{N}_{\mathrm{NH_3}}|_{\mathrm{l}}$ with Eq. (1).
(5) If $\Delta\dot{N}_{\mathrm{NH_3}}|_{\mathrm{v}} - \Delta\dot{N}_{\mathrm{NH_3}}|_{\mathrm{l}} = 0$ go to sep (6), otherwise guess a new value of z and go to step (4).
(6) Calculate the modified heat transfer coefficients with Eqs. (9) and (11).
(7) If Eq. (10) is verified go to step (8), otherwise guess a new value of T_{i} and go to step (2).
(8) Calculate the mass fluxes $\Delta\dot{M}_{\mathrm{NH_3}}$ and $\Delta\dot{M}$ with Eqs. (3) and (4). The new flow and concentration of the vapour current can be determined with Eqs. (15) and (16), and for the liquid current using Eqs. (12) and (13).
(9) With $\Delta\dot{q}_{\mathrm{v}}$ and $\Delta\dot{q}_{\mathrm{l}}$ calculate the enthalpy of the liquid and vapour phases for the next section, using Eqs. (14) and (17).

3.2. Distillation column

In the model of the distillation column the following parameters are considered: geometry of the column (its diameter and the stripping and rectifying lengths), packing features (material, specific area, packing factor, number of elements per volume) and operating characteristics and requirements such as, feed inlet conditions (mass flow, concentration and temperature), distillate mass flow, condensation temperature and condensate subcooling, heat load in the generator and volumetric heat rejection in the rectifying and stripping sections.

In order to apply the previous algorithm to solve the distillation column the liquid and vapour conditions at any section must be known. Thus, another iterative procedure has to be established, based on global mass, species and energy balances around the column and the condenser. The calculation procedure begins by assuming vapour distillate temperature and concentration. Subsequently the column pressure is determined, since the temperature and subcooling of the condensate are known. Eqs. (18) and (19) are used to obtain the mass flow and concentration of the bottom product and the temperature and concentration of the generated vapour. The heat rejected from the condenser can now be calculated using Eq. (20) and with Eq. (21) the vapour flow at the top of the column is computed.

$$\dot{m}_{\mathrm{F}} = \dot{m}_{\mathrm{D}} + \dot{m}_{\mathrm{B}} \tag{18}$$

$$\dot{m}_{\mathrm{F}} \cdot x_{\mathrm{F}} = \dot{m}_{\mathrm{D}} \cdot x_{\mathrm{D}} + \dot{m}_{\mathrm{B}} \cdot x_{\mathrm{B}} \tag{19}$$

$$\dot{m}_{\mathrm{F}} \cdot h_{\mathrm{F}} + \dot{Q}_{\mathrm{G}} = \dot{m}_{\mathrm{D}} \cdot h_{\mathrm{D}} + \dot{m}_{\mathrm{B}} \cdot h_{\mathrm{B}} + \dot{Q}_{\mathrm{C}} \tag{20}$$

$$\dot{Q}_{\mathrm{C}} = \dot{m}_{\mathrm{v,top}} \cdot h_{\mathrm{v,top}} - (\dot{m}_{\mathrm{v,top}} - \dot{m}_{\mathrm{D}}) \cdot h_{\mathrm{D}} \tag{21}$$

Once the conditions at the top of the column are known, the procedure described in the previous section can be used in each incremental element in the rectifying section marching in downwards direction. At the feed entry point the liquid and vapour fractions of the feed flow are considered to mix with the downward liquid from the rectifying zone and with the upward vapour from the stripping zone, respectively. Therefore, the liquid and vapour conditions at the upper section of the stripping zone are known. Hereafter the stripping zone can be calculated as stated before. Thus, the conditions at the bottom of the column are obtained and the temperature and concentration of the vapour phase are compared with the generator temperature and the corresponding vapour equilibrium concentration. If the calculated values are different, a new guess for the distillate temperature and concentration is made. Finally, the correlation reported by Eckert [29] is used to determine the flooding velocity in all of the incremental elements, in order to verify that flooding operation is not attained.

The solution method explained above has been implemented in a computer program using FORTRAN 90.

4. Results and discussion

The implemented model has been used to simulate and to analyse the performance of distillation columns. The computer program results predict the behaviour of a distillation column for a given geometry, packing type and operating conditions. Furthermore, a parametric study was carried out in order to analyse the influence of each parameter on the column performance and behaviour. Results for a specific application are presented here.

The sample data required by the program and used to obtain the presented results are specified in Table 1. Packing features are enumerated in Table 2. These data characterise representative design and operating conditions of a distillation column for a small capacity ammonia–water absorption refrigeration system. Direct numerical results of the column operation are presented in Table 3. Likewise, the temperature, concentration and mass flow distributions for the liquid and vapour streams, as well as the mass and heat transferred throughout the column are obtained.

Table 1
Operating conditions and geometry of the column

Feed flow (kg·s^{-1})	0.0208
Feed concentration (kg·kg^{-1})	0.42
Feed temperature (K)	343
Distillate flow (kg·s^{-1})	0.00347
Generator heat load (kW)	10
Condensation temperature (K)	303
Condensate subcooling (K)	0
Volumetric heat rejection (kW·m^{-3})	0
Rectifying length (m)	0.4
Stripping length (m)	0.4
Rectifying diameter (m)	0.06
Stripping diameter (m)	0.1

Table 2
Packing features

	Rectifying	Stripping
Type	Berl saddles $\frac{1}{4}''$	Berl saddles $\frac{1}{2}''$
Material	Ceramic	Ceramic
Surface area (m^2·m^{-3})	900	465
Packing factor (m^{-1})	2950	790
Elements (per m^3)	3779000	590000

Table 3
Results

Distillate concentration (kg·kg^{-1})	0.9985
Pressure (bar)	11.64
Bottoms flow (kg·s^{-1})	0.0173
Bottoms concentration (kg·kg^{-1})	0.30
Bottoms temperature (K)	380
Top vapour flow (kg·s^{-1})	0.0054
Top vapour temperature (K)	313
Reflux flow (kg·s^{-1})	0.0019
Reflux ratio	0.35

Fig. 3 shows temperature profiles along the distillation column length. The vapour temperature decreases from the bottom (generation temperature) to the top of the column, while the liquid solution temperature increases as it flows down through the column. An abrupt temperature change can be observed in the liquid temperature profile at the column feed point, due to the difference in temperature of the liquid leaving the rectifying section and the liquid feed temperature. Fig. 3 also shows that the bulk liquid temperature is very close to the interface temperature, while the bulk vapour temperature is somewhat higher than the equilibrium temperature. This denotes that heat transfer resistance is dominant in the vapour rather than in the liquid phase.

Fig. 4 indicates ammonia mass concentration profiles at different lengths in the distillation column. The bulk vapour concentration increases as the vapour rises through the column and is always lower than the equilibrium vapour concentration at the interface. On the other hand, the liquid

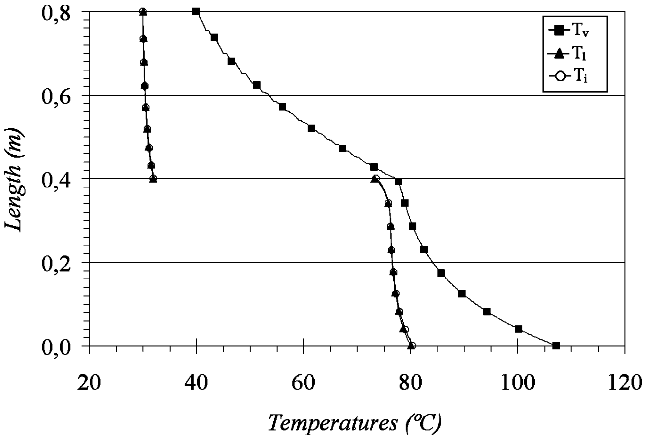

Fig. 3. Temperature profiles along the length of the distillation column.

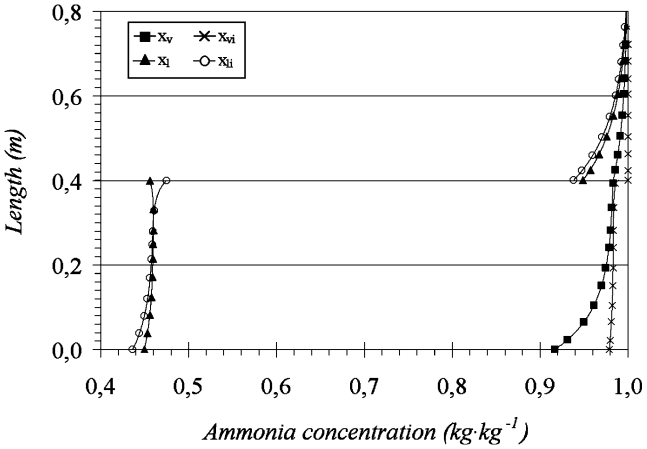

Fig. 4. Ammonia concentration profiles along the length of the distillation column.

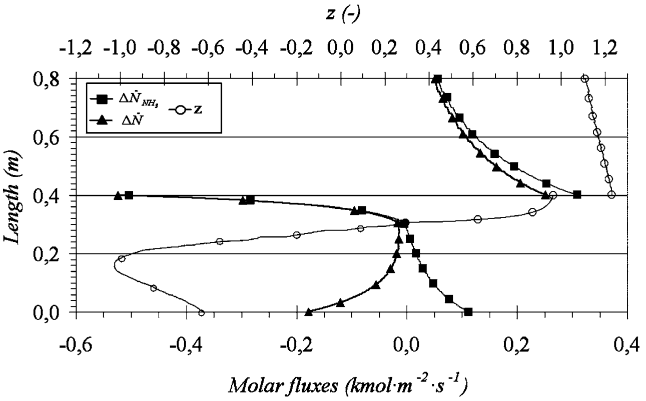

Fig. 5. Ammonia molar flux, net molar flux and ratio z along the length of the distillation column.

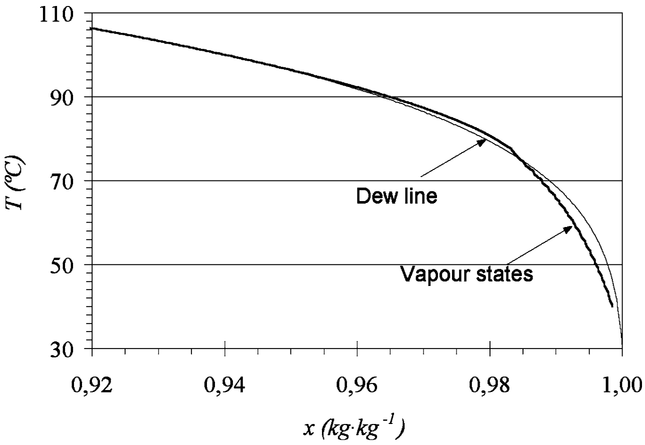

Fig. 6. Vapour state evolution along the column in a T–x diagram.

solution becomes poorer in ammonia content as it descends in the column. The liquid solution at the bottom of the stripping section is different from the liquid solution leaving the generator, therefore the liquid concentration value at the bottom of the stripping section, represented in Fig. 4, does not match the bottoms concentration in Table 3. The interface liquid concentration is somewhat lower than the bulk liquid concentration. The predictions of the model in the stripping section next to the column feed entry point are noteworthy. Results in Fig. 4 reflect that the bulk liquid concentration increases and is lower than the equilibrium liquid concentration. This is due to the subcooling state of the column feed in the case under study. It may also be concluded from Fig. 4 that mass transfer resistance is dominant in the vapour region, since the bulk and the interface liquid concentration are very close throughout the column.

Fig. 5 shows the total and ammonia molar flux profiles along the column length. The ratio of ammonia molar flux to the total molar flux transferred, z, was also obtained and is also presented in Fig. 5. In the rectifying section ammonia is desorbed into the vapour region, while water is absorbed by the liquid. Consequently, the total molar flux is lower than the ammonia molar flux, therefore the ratio z is greater than 1. At the top of the rectifying section the ratio z approaches unity since the liquid and vapour solutions are nearly pure ammonia. In the stripping section, next to the column feed point, the liquid is subcooled, as pointed out before. The results show that ammonia and water are absorbed by the liquid phase. Thus, the ratio z is lower than 1 and is between the liquid and vapour equilibrium concentrations at the interface. Since the water concentration of the mass transferred from the vapour to the liquid is higher than the bulk vapour concentration, the vapour increases its ammonia concentration in this zone. In the stripping section, downstream from the column feed entry point, ammonia is desorbed into the vapour phase while water is absorbed into the liquid resulting in a net molar flux from the vapour to the liquid phase. This implies that the ratio z is lower than zero, so that the vapour is enriched in ammonia, as can be seen in Figs. 3 and 5.

Fig. 6 shows the vapour state evolution as it rises in the distillation column on a temperature versus concentration diagram. The model predicts that the bulk vapour states are close to saturation conditions in the stripping section, while in the rectifying section, the vapour temperature and concentration is slightly below the dew point line, as shown in this figure. Nevertheless, as the vapour ammonia concentration approaches unity, the dew line is much steeper and the vapour phase is closer to the saturation conditions.

Parametric studies were conducted to investigate the effect of geometric and operating design parameters on the distillation column behaviour. Each parameter has been varied while keeping all other geometric and operating data constant. The influence of rectifying and stripping lengths and mass and heat transfer coefficients on the distillate ammonia concentration is shown next, considering the remaining parameter values in Tables 1 and 2 as constant. Moreover the effects of a volumetric heat rejection from the column is also analysed.

Fig. 7 shows distillate ammonia content as a function of rectifying and stripping lengths for a constant total column length of 0.8 m. Increasing the packing length dedicated to rectification results in a higher distillate concentration. However, a maximum value is obtained around rectification length of 0.7 m and stripping length of 0.1 m. This is reasonable because the liquid flow and the vapour concentration gradients in the stripping section are higher than in the rectifying section.

Fig. 8 shows the effect of heat and mass transfer coefficients in the liquid and vapour regions on the ammonia concentration of the distillate vapour. The horizontal axis represents the multiplying factor of the transfer coefficients which was varied from 0.5 to 2. The vapour mass transfer coefficient influences considerably the distillate concentration while the heat transfer coefficients and the liquid mass transfer coefficient have no significant effect. Increasing the

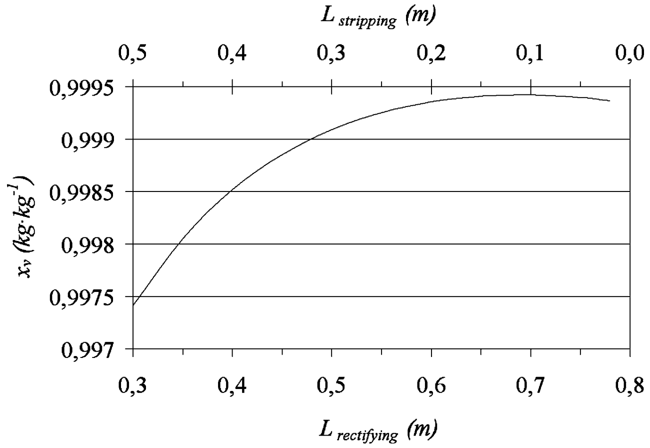

Fig. 7. The effect of the stripping and rectifying sections lengths on the distillate ammonia concentration, considering a constant column length of 0.8 m.

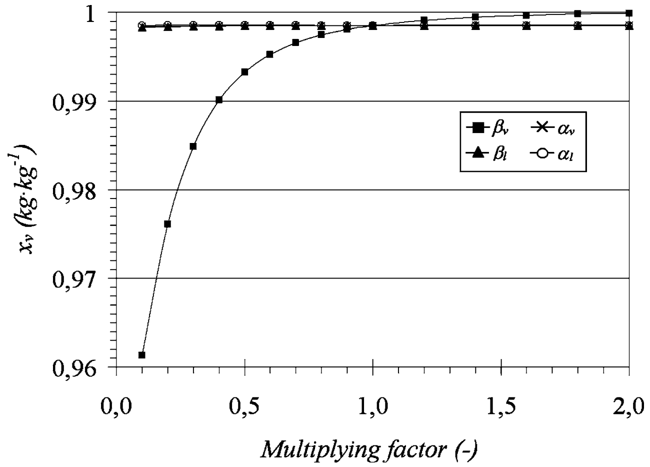

Fig. 8. Effect of the heat and mass transfer coefficients on the distillate ammonia concentration.

vapour mass transfer coefficient results on substantial augmentation of the distillate concentration or a smaller column length to achieve a specific separation.

The effect of varying the heat rejection from the column was also studied. When increasing the heat rejection from the column, a higher rate of vapour condensation was observed, resulting in a lower rate of ammonia desorbed from the liquid phase. For higher values, water and ammonia absorption was obtained throughout the whole column. Fig. 9 shows the effect of the volumetric heat rejection from the packing on the water content of the distillate vapour. As the heat rejection from the column increases the water content of the distillate vapour decreases, but to rise the vapour ammonia concentration from 0.9985 to 0.9989 as much as 6 kW must be rejected from the column. This result lead to the conclusion that if a high ammonia purification process is desired it is not worthy complicating the column design for a heat rejection function.

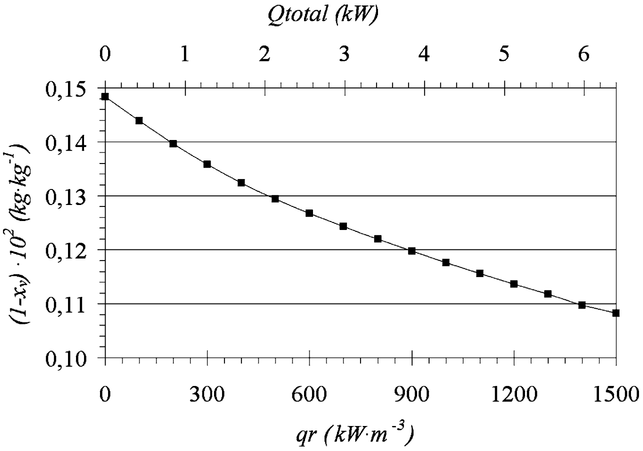

Fig. 9. Effect of the volumetric heat rejection (or total heat rejected from the column) on the distillate water concentration.

5. Conclusions

In this paper a two film model based on combined heat and mass transfer processes of a packed distillation column in an ammonia–water absorption refrigeration system has been described. Because the heats of vaporization of ammonia and water are different, a net molar flux is transferred at the interface and equimolar counter diffusion has not been considered, as confirmed in the results presented in the paper. Solution of simultaneous heat and mass transfer equations showed that interface temperature is nearly equal to the bulk liquid temperature and that liquid mass transfer resistance is negligible. The model was applied to find the optimal stripping and rectifying lengths for a given geometric design parameters and operating conditions, obtaining that the required rectifying section is much longer than the stripping section. The vapour mass transfer coefficient was found to have the most significant effect on the distillate ammonia concentration, while the influence of other transfer coefficients is negligible. Finally the effect of a volumetric heat rejection from the column was shown to have a slight influence on the distillation column performance.

References

[1] F. Ziegler, Recent developments and future prospects of sorption heat pump systems, Internat. J. Therm. Sci. 38 (1999) 191–208.
[2] M.J.P. Bogart, Pitfalls in ammonia absorption refrigeration, Internat. J. Refrig. 4 (1982) 203–208.
[3] K. Stephan, History of absorption heat pumps and working pair developments in Europe, Internat. J. Refrig. 3 (1983).
[4] R. Moller, K. Knoche, Surfactants with NH_3–H_2O, Internat. J. Refrig. 19 (1996) 317–321.
[5] F. Ziegler, S. Grossman, Heat transfer enhancement by additives, Internat. J. Refrig. 19 (1996) 301–309.
[6] V.G. Balmuru, O.M. Ibrahim, S.M. Barnett, Simulation of ternary ammonia–water–salt absorption refrigeration cycles, Internat. J. Refrig. 23 (2000) 31–42.
[7] K.E. Herold, R. Radermacher, S.A. Klein, Absorption Chillers and Heat Pumps, CRC Press, 1996.

[8] M.J.P. Bogart, Ammonia Absorption Refrigeration in Industrial Processes, Gulf Publishing Company, Houston, TX, 1981.

[9] W.L. McCabe, J.C. Smith, P. Harriott, Unit Operations of Chemical Engineering, McGraw-Hill, 1993.

[10] A.P. Colburn, T.B. Drew, The condensation of mixed vapors, AIChE Trans. 33 (1937).

[11] P.D. Iedema, S.H. Liem, B. Van der Wekken, Heat and mass transfer in vapour and liquid phases of a H_2O/NH_3—regenerator, in: Proceedings of 15th International Congress of Refrigeration, Commission E2, Trondheim, 1985.

[12] Y.T. Kang, R.N. Christensen, Development of a counter-current model for a vertical fluted tube GAX absorber, in: International Absorption Heat Pump Conference, 31, 1993.

[13] Y.T. Kang, W. Chen, R.N. Christensen, A generalized component design model by combined heat and mass transfer analysis in NH3–H2O absorption heat pump systems, ASHRAE Trans. 103 (1997).

[14] Y.T. Kang, W. Chen, R.N. Christensen, Design of ammonia–water condenser with a fluted tube, ASHRAE Trans. 102 (1996).

[15] Y.T. Kang, W. Chen, R.N. Christensen, Development of design model for a rectifier in GAX absorption heat pump systems, ASHRAE Trans. 102 (1996).

[16] Y.T. Kang, R.N. Christensen, T. Kashiwagi, Ammonia–water bubble absorber with a plate heat exchanger, ASHRAE Trans. 104 (1998).

[17] J. Cao, R.N. Christensen, Comparison of binary mixture heat and mass transfer analysis with single-component heat and mass transfer analysis in the design of GAX absorber/desorber, ASHRAE Trans. 106 (2000).

[18] A.M. Selim, M.M. Elsayed, Interfacial mass transfer and mass transfer coefficient in aqua ammonia packed bed absorber, Internat. J. Refrig. 22 (1999) 263–274.

[19] A.M. Selim, M.M. Elsayed, Performance of a packed bed absorber for aqua ammonia absorption refrigeration system, Internat. J. Refrig. 22 (1999) 283–292.

[20] W.K. Lewis, W.G. Whitman, Ind. Engrg. Chem. 1 (1924) 1215.

[21] R.B. Bird, W.E. Steward, E.N. Lightfoot, Transport Phenomena, John Wiley & Sons, New York, 1960.

[22] R.E. Treybal, Mass Transfer Operations, McGraw-Hill, 1980.

[23] D.R. Webb, Condensation of vapour mixtures, in: Heat Exchanger Design Handbook, Begell House, 1998.

[24] K. Onda, H. Takeuchi, Y. Okumoto, J. Chem. Engrg. Jpn. 1 (1968) 56.

[25] P.V. Danckwerts, Gas-Liquid Reactions, McGraw-Hill, 1970.

[26] R. Zarzychi, A. Chacuk, Absorption Fundamentals and Applications, Pergamon Press, 1993.

[27] T.H. Chilton, A.P. Colburn, Ind. Engrg. Chem. 26 (1934).

[28] B. Ziegler, Ch. Trep, Equation of state of ammonia–water mixtures, Internat. J. Refrig. 7 (1984) 101–106.

[29] J.S. Eckert, Chem. Engrg. Prog. 66 (1970).